Journal of Applied Polymer Science

Synthesis of End-Functionalized Poly(*N*-isopropyl acrylamide) with Zinc Porphyrin and Its Photocatalytic Activity Under Visible Light

Nannan Qiu,[1] Yanhui Li,[1] Shuangli Han,[2] Toshifumi Satoh,[3] Toyoji Kakuchi,[3] Qian Duan[1]

[1]School of Materials Science and Engineering, Changchun University of Science and Technology, Changchun 130022, China
[2]Changchun Institute of Optics, Fine Mechanics, and Physics, Chinese Academy of Sciences, Changchun 130033, China
[3]Division of Biotechnology and Macromolecular Chemistry, Graduate School of Engineering, Hokkaido University, Sapporo 060-8628, Japan
Correspondence to: Q. Duan (E-mail: duanqian88@hotmail.com)

ABSTRACT: A series of well-defined linear poly(*N*-isopropyl acrylamide) with an asymmetrical zinc(II) porphyrin (ZnPor–PAM) end group was synthesized by atom transfer radical polymerization, wherein 5,10,15,20-*tetra*(*p*-bromopropanoyloxyethylphenyl) zinc porphyrin tripropionate was used as the initiator and CuBr/tris(2-dimeoethyl)amine was used as the catalyst system. The structure of the ZnPor–PAM was characterized by Fourier transform infrared spectroscopy and ^{1}H-NMR. In addition, the polydispersity index (PDI) obtained by gel permeation chromatography indicated that the molecular weight distribution was narrow; thus, the polymerization was well controlled ($1.05 < \text{PDI} < 1.21$). Because of the incorporation of hydrophobic porphyrin, the lower critical solution temperature of ZnPor–PAM was lower than that of the *N*-isopropyl acrylamide homopolymer. Most interestingly, the ZnPor–PAM possessed remarkable photocatalytic activity for the oxidative degradation of methylene blue in the presence of hydrogen peroxide under visible-light radiation. Moreover, ZnPor–PAM could be reused through the uncomplicated procedure, which exploited the thermoresponsive properties of ZnPor–PAM without any significant loss in activity. © 2014 Wiley Periodicals, Inc. J. Appl. Polym. Sci. **2014**, *131*, 40523.

KEYWORDS: catalysts; functionalization of polymers; photochemistry; recycling; stimuli-sensitive polymers

Received 18 November 2013; accepted 27 January 2014
DOI: 10.1002/app.40523

INTRODUCTION

Environmental pollution has become the major problem and has received increasing attention in current scientific research. In particular, about 15% of the total production of dyes is lost during the dyeing process and is released in textile effluents. Their variety, toxicity, and persistence of dyes directly impact the health of ecosystems and present an immediate threat to human beings via their contamination of drinking water supplies.[1] To cope with this serious problem, research interest has been placed on establishing alternative, simple, low-cost technologies for the on-site treatment of wastewaters.[2] There are a significant number of dye removal methods, including biological, physical, and chemical methods.[3,4] In recent years, advanced oxidation processes (AOPs) based on the generation of reactive species have been proposed to quickly and nonselectively oxidize a broad range of organic pollutants.[5,6] Among the new oxidation methods or AOPs, photocatalytic oxidative treatments are usually most effective in the destruction of the chromophoric structures of dyes.[7]

In the field of photocatalytic oxidation, metalloporphyrins have attracted considerable attention because of their high electron transfer abilities and redox properties. Several synthetic metalloporphyrin derivatives with various structures and core metals have shown high photocatalytic activity and are environmentally friendly in the activation of molecular O_2 or hydrogen peroxide (H_2O_2) in the degradation of organic pollutants.[8–10] However, their applications are restricted by the following problems: poor solubility, high tendency to agglomerate and difficult recycling after the catalytic process. In response, the poor solubility in solution, especially in water, could be improved through the incorporation of a suitable substitute on the peripheral circle of porphyrin. Immobilizing the porphyrin complexes onto insoluble solid substrates can prevent the formation of agglomerates and facilitate the recycling of the catalyst, but there are several shortcomings in these strategies. For instance, the substituting groups are limited, the transmittance is decreased, and the system of photocatalytic degradation is the heterogeneous phase. It is well known that heterogeneous photocatalysis can lead to the mineralization of most organic pollutants, but the degradation

Additional Supporting Information may be found in the online version of this article.

effect will be better if the photocatalytic degradation is processed in a homogeneous photocatalytic system.[11] Thus, it is of great significance to develop a water-soluble photocatalyst which can exhibit efficient performance in the homogeneous system and also can be recycled effectively preventing secondary pollution.

Poly(*N*-isopropyl acrylamide) (PNIPAM) is a well-known thermoresponsive polymer, which exhibits a coil–globule transition in aqueous solutions at a lower critical solution temperature (LCST) of 32°C.[12–14] A great deal of attention has been focused on the thermoresponsive properties of various functional polymers consisting of PNIPAM for their extensive applications, such as drug-delivery systems and photocatalytic processes.[15–20] In recent years, PNIPAM has been synthesized through controlled/living radical polymerization (CRP), which provides an efficient way of synthesizing polymers with a designated structure and chemical composition. Atom transfer radical polymerization (ATRP) is one of the most investigated CRP processes. It can control polymers with a more narrow molecular weight distribution compared to other CRP methods, such as reversible addition–fragmentation chain transfer and nitroxide-mediated radical polymerization.[21–24] Thus, our group has synthesized several end-functionalized PNIPAMs via ATRP and investigated their thermoresponsive properties.[25–27] Recently, we also studied the photocatalytic degradation of PNIPAM with asymmetrical phthalocyanine, but the preparation process of asymmetrical phthalocyanine is more complex, and the production rate is lower compared with that of porphyrin.[28]

In this study, we synthesized a series of well-defined linear PNIPAMs with an asymmetrical zinc(II) porphyrin (ZnPor–PAM) end group via ATRP. The photocatalytic activity was tested on the basis of the oxidative degradation of methylene blue, and recycling experiments were also conducted. The results indicate that the ZnPor–PAMs possessed favorable photocatalytic activity and could be conveniently recycled after the catalytic process.

EXPERIMENTAL

Materials

N-Isopropyl acrylamide (NIPAM; 99%, Aldrich) was recrystallized twice from benzene/hexane (10:1 v/v) before use. The CuBr (99%, Aldrich) catalyst was washed successively with acetic acid, dried with ether, and then stored under a nitrogen atmosphere. Tris[2-(dimethylamino)ethyl]amine (Me_6TREN) was synthesized according to the literature.[29] *p*-hydroxybenzaldehyde (99%, Aldrich), 2-bromoethyl alcohol (99%, Aldrich), zinc acetate (99%, Aldrich), and 2-bromopropionyl bromide were used as received (99%). All other chemicals were purchased from Sinopharm Chemical Reagent Co. and were used as received.

Measurements

^{1}H-NMR spectra were measured on a Bruker Avance 400-MHz spectrometer at room temperature with $CDCl_3$ as the solvent. Element analysis was performed with a Carlo Erba-MOD1106 instrument. The molecular weights (The number-average molecular weight is gotten by GPC ($M_{n,GPC}$)) and polydispersity index [PDI: weight-average molecular weight (M_w)/number-average molecular weight (M_n)] were measured with gel permeation chromatography (GPC) with a Waters e2695 separation module, two waters Styragel columns (HR4 and HT3, 300 × 7.8 mm^2, 5 μm particles, exclusion limits = 5000–30,000 and 500–30,000 g/mol, respectively), and a Waters 2414 refractive index detector maintained at 35°C. The polymer molar masses were determined with linear polystyrene as calibration standards. Tetrahydrofuran (THF) was used as a mobile phase at a flow rate of 1.0 mL/min. We obtained Fourier transform infrared spectra by measuring samples in KBr disks on a Shimadzu IR-8400S spectrometer. Ultraviolet–visible (UV–vis) spectra were measured on a UV Mini 1240 (Shimadzu) spectrophotometer.

Photocatalytic Degradation of Methylene Blue Catalyzed by ZnPor–PAM

ZnPor–PAM and H_2O_2 were added to an aqueous solution of methylene blue, and the mixture was stirred for 15 min before it was exposed to light irradiation. Then, the catalytic system containing the catalyst, H_2O_2, and methylene blue was irradiated by a 500-W halogen lamp through a glass filter (the wavelength of the light source (λ) > 450 nm), during which the degradation of methylene blue was determined from changes in the absorbance on samples (3 mL) obtained at different irradiating intervals on a UV–vis spectrometer. In addition, the pH value of the solution was adjusted through the addition of standard buffer solutions, and the initial concentration of methylene blue solution was 4 × 10^{-5} mol/L.

The rate of degradation (D) of methylene blue can be defined as follows:

$$D=(A_0-A)/A_0\times 100\%$$

where A_0 is the initial absorption intensity at 665 nm and A is the absorption intensity at any time during the measurement.

Synthesis of the End-Functionalized ZnPor–PAM (Scheme 1)

The preparation procedures of 5,10,15,20-*tetra*(*p*-hydroxyethylphenyl) zinc porphyrin tripropionate (ZnPor–OH) and 5,10,15,20-*tetra*(*p*-bromopropanoyloxyethylphenyl) zinc porphyrin tripropionate (ZnPor–Br) are depicted in the Supporting Information (Schemes S1 and S2).

ZnPor- PAM were synthesized as followed (S1): NIPAM (448 mg, 4.00 mmol), CuBr (31.9 mg, 0.16 mmol), and Me_6TREN (39 μL, 0.16 mmol) were dissolved in 2 mL of dimethylformamide (DMF)/water (2:1 v/v). This was followed by degassing via three freeze–pump–thaw cycles. A deoxygenated solution of ZnPor–Br (25.6 mg, 0.02 mmol) in DMF (0.5 mL) was then added to the reaction ask to start the polymerization. The reaction was carried out for 12 h at 60°C under a nitrogen atmosphere. Polymerization was terminated by exposure to air. Then, the reaction mixture was diluted with THF and passed through an alumina column (S1). The resulting polymer was purified by dialysis with a cellophane tube (molecular weight cutoff = 2000) in DMF.

IR (cm^{-1}): 3295 (ν_{N-H}), 1750 ($\nu_{C=O}$), 2850–2960 ($\nu_{-CH2,-CH3}$), 1650 ($\nu_{C=O}$), 1550 (δ_{C-H-N}), 960, 990 (skeletal vibration of pyrrole; Supporting Information, Figure S3B). ^{1}H-NMR (400 MHz, $CDCl_3$, δ): 8.86 (s, 8H), 8.11 (d, 8H), 7.27 (d, 8H), 6.20

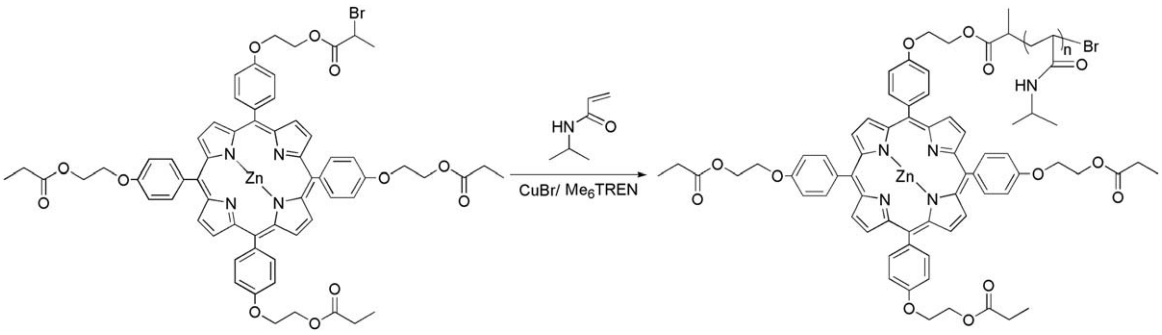

Scheme 1. Synthesis route for ZnPor–PAM.

(s, 68H), 4.04 (m, 68H), 2.21 (t, 68H), 1.62 (d, 136H), 1.15 (d, 410H; Supporting Information, Figure S4B).

RESULTS AND DISCUSSION

Synthesis and Characterization

Well-defined linear ZnPor–PAM was successfully prepared via ATRP with ZnPor–Br as the initiator and CuBr/Me_6TREN as the catalyst system. Figure S3(B) in the Supporting Information shows the IR spectra of ZnPor–PAM. The characteristic absorptions of PNIPAM were clearly observed, as evidenced by the presence of a carbonyl stretching vibration ($\upsilon_{C=O}$) at 1650 cm^{-1} and the N—H bending vibration (δ_{N-H}) at 1550 cm^{-1}. The strong absorbance at 3304 cm^{-1} was assigned to the stretching vibrations (υ_{N-H}) of the acylamino group. Obviously, the characteristic peaks of the porphyrin skeleton could not be resolved clearly in the Fourier transform infrared spectra. Next, the structure was further confirmed by ^{1}H-NMR (Supporting Information, Figure S4B). The signals at 8.92, 8.43, and 7.72 ppm were attributed to the protons on the porphyrin core. The signals at 6.76, 4.0, 3.12, 1.94, and 1.16 ppm were assigned to the protons on the repeated units of NIPAM. In addition, the molecular weight of ZnPor–PAM ($M_{n,GPC} = 7800$) determined by ^{1}H-NMR analysis was 7770, which was consistent with the GPC results.

The M_n values of the ZnPor–PAM were determined by GPC with polystyrene as the standard. The results are presented in Table I, and the GPC traces of ZnPor–PAM are shown in Figure 1. There was no tailing at either side. This suggested the absence of any small molecules, such as initiator, monomer, or other byproduct residues. Moreover, the PDIs of the polymers were relatively narrow ($M_w/M_n = 1.05$–1.21), which demonstrated that the polymerization was a living and controlled process.

The UV–vis spectra of ZnPor–Br and ZnPor–PAM showed the B-band characteristic of ZnPor–Br at 416 nm and those of Q bands at 548 and 591 nm [Figure 2(a)], which were in accordance with those observed for similar metalloporphyrins.[30] Moreover, the B-band absorption of ZnPor–PAM at 423 nm and the Q-bands absorptions at 562 and 606 nm exhibited a bathochromic shift relative to the bands of ZnPor–Br. This was due to the fact that PNIPAM arms took the place of the electron-withdrawing group (—Br), which made the forbidden bandwidth narrow, and the electrons were easily inspired, so the transition absorption band of π–π^* moved to the long wave. In addition, the solubility of ZnPor–PAM was improved, and this demonstrated its ability to be dissolved in water and common organic solvents. Figure 2(b) indicates that the UV–vis spectrum of ZnPor–PAM did not exhibit any changes other than an increase in intensity as the concentration of ZnPor–PAM was gradually increased from 0.05 to 0.4 mol/L. Thus, we concluded that ZnPor–PAM exhibited high solubility and good stability in aqueous solutions with the incorporation of PNIPAM.

Thermoresponsive Properties of ZnPor–PAM

UV–vis spectroscopy was investigated to determine the LCST of the ZnPor–PAM aqueous solution. When the temperature was lower than the LCST, ZnPor–PAM had good solubility in water; when the temperature was higher than the LCST, its macromolecules experienced dehydration and collapsed from a hydrated, extended coil to a hydrophobic globule, and the solution

Table I. Data of the Polymerization Reactions and the LCSTs of the ZnPor–PAM Samples

Run	Reaction time (h)	Concentration (%)[a]	M_n[b]	M_w[b]	M_w/M_n	LCST (°C)[c]
1	2	15	2300	2420	1.05	
2	5	37	4050	4410	1.09	26.5
3	8	50	6030	6750	1.12	28.0
4	12	65	7800	8890	1.14	29.5
5	16	80	10,300	12,270	1.19	31.0
6	20	89	13,000	15,730	1.21	31.5

[a] Determined by gravimetric measurements.
[b] Determined by GPC with THF as the eluent with respect to polystyrene standards.
[c] Measured by turbidimetry with a UV-vis spectrophotometer.

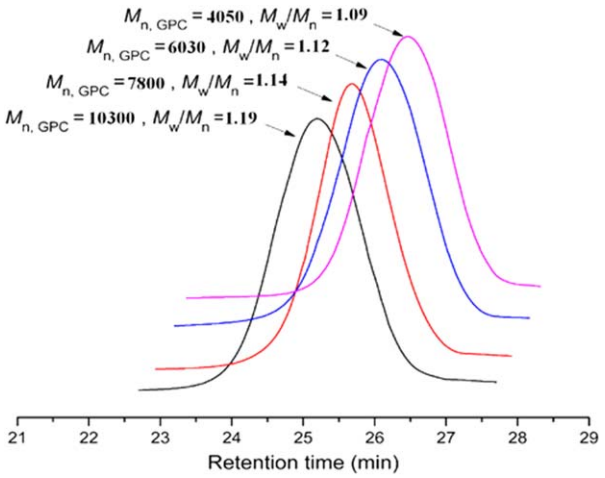

Figure 1. GPC traces of ZnPor–PAM. [Color figure can be viewed in the online issue, which is available at wileyonlinelibrary.com.]

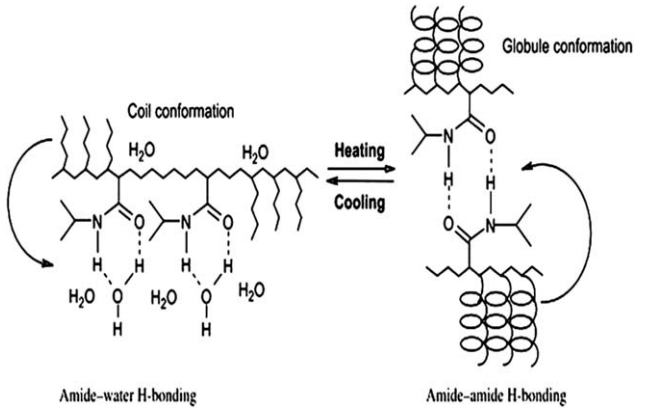

Figure 3. Scheme for the thermosensitive properties of PNIPAM.

gradually turned turbid (Figure 3). Figure 4 represents the curves of transmittance with increasing temperature; this revealed the temperature dependence of optical transmittance at 500 nm for the polymer aqueous solution. With increasing temperature, the optical transmittance showed little change during the first step. When the temperature was lower than the LCST, the hydrogen bonding interaction between the amido of polymers and water molecules made the polymers show good solubility in water. However, when the temperature continued to increase, the strong association interaction between hydrophobic isopropyl may have inhibited the formation of hydrogen bonds between the amido groups of the polymers and water molecules, and a repulsive force from the increased hydrophobicity of micelles may have caused large aggregates and a decrease in the optical transmittance. The LCST value is defined as the temperature producing a 10% decrease in the transmittance at an optical transmittance at 500 nm. The LCST values of the aqueous solutions of various polymers are listed in Table I. Obviously, the LCSTs of the various polymers were lower than that of the NIPAM homopolymer, and this was consistent with reports in which the hydrophobic groups decreased the thermal phase-transition temperature of PNIPAM.[31] In addition, the LCSTs of the various polymers gradually approached 32°C with increasing molecular weight. This was attributed to the effect of porphyrin on the performance of the polymer, which became weaker when the proportion of porphyrin in the polymer chain was lowered with increasing molecular weight. On the contrary, the ZnPor–PAM with the $M_{n,GPC}$ of 2300 could not dissolve in water because of the critical effect of the hydrophobic porphyrin.

Photocatalytic Activity of ZnPor–PAM on Methylene Blue

The degradation of methylene blue with H_2O_2 as an oxidant and metalloporphyrin as a catalyst may have involved two mechanisms. On the one hand, zinc porphyrins (ZnPor's) acted as photosensitizers to activate $^3O_2$ into active $^1O_2$ under light irradiation; then, the substrate was subsequently oxidated by the active $^1O_2$.[32] On the other hand, under visible-light irradiation, the ground-state ZnPor was excited to its excited state via one photon transition. Then, the photoinduced electrons could be trapped by adsorbed H_2O_2 or O_2 to produce reactive species ·OH quickly. Finally, the ·OH could photodegrade the methylene blue efficiently.[33,34]

To investigate the catalytic performance of ZnPor–PAM under visible-light irradiation, we carried out a series photodegradation

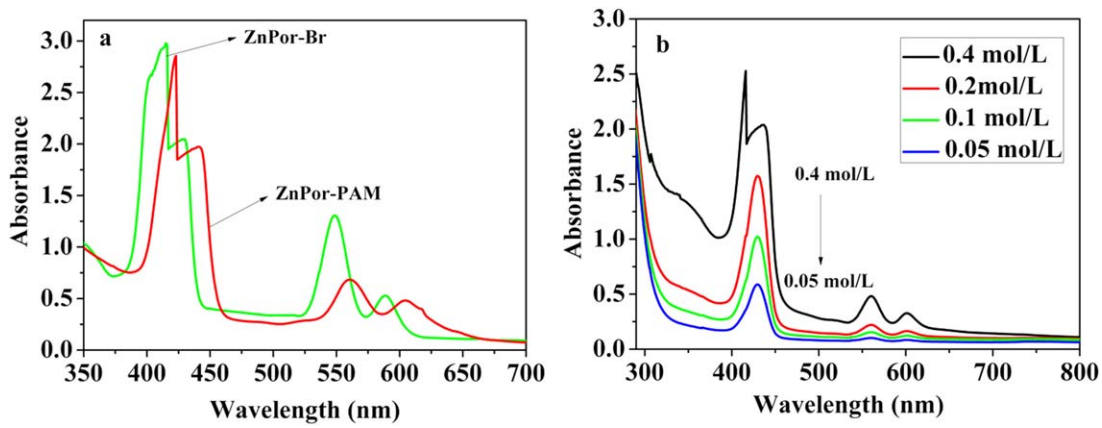

Figure 2. (a) UV–vis spectra of ZnPor–Br and ZnPor–PAM (M_n = 7800) in CH_2Cl_2 (0.4 mol/L) and (b) UV–vis spectra of ZnPor–PAM (M_n = 7800) in aqueous solutions with different concentrations. [Color figure can be viewed in the online issue, which is available at wileyonlinelibrary.com.]

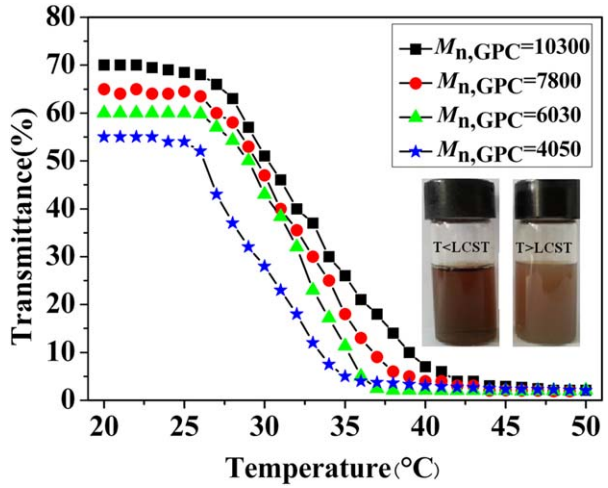

Figure 4. Temperature dependence of the optical transmittance at 500 nm for aqueous solutions of ZnPor–PAM with a concentration of 2 mg/mL. [Color figure can be viewed in the online issue, which is available at wileyonlinelibrary.com.]

experiments of methylene blue, which is a kind of commercial nonbiodegradable toxic dye with an aromatic structure. Figure 5 shows that methylene blue was hardly degraded in only the presence of ZnPor–PAM with visible light (curve D) or ZnPor–PAM with H_2O_2 (curve C). However, H_2O_2 with visible light (curve B) indicated that methylene blue was degraded by a mere 10%, and ZnPor–OH with H_2O_2 and visible light (curve E) showed a slightly higher degradation rate of 20%. From the results, we concluded that ZnPor–OH showed a certain photocatalytic activity, but the effect was very weak because of the suspension of ZnPor–OH in the catalytic systems without dissolution. Finally, we observed that more than 75% of methylene blue was degraded according to ZnPor–PAM with H_2O_2 and visible light (curve A) after 180 min. The results demonstrate that ZnPor–PAM, H_2O_2 and visible light had a strong interaction that was essential for the degradation of methylene blue. What is more, ZnPor–PAM could be dissolved in water by the immobilization of the porphyrin onto PNIPAM. This allowed for the entire photocatalytic degradation process to be carried out in a homogeneous system, which greatly improved the catalytic efficiency.

To study the relationship between the *D* and pH values, we performed the experiments of photocatalytic degradation under various different pHs, and the results are shown in Figure 6(a). At a pH value of 1, the degradation rate merely reached 67% after 3 h and increased gradually with pH. At a pH value of 2, the degradation rate reached 91% because of the increase in the concentration of HO· with the enhancement in ionization; this was beneficial for the oxidation of the substrate. Thus, the degradation rate increased significantly. However, the degradation rate gradually decreased as the pH continued to rise, reaching 20% at a pH value of 8. This behavior was attributed to the fact that excessive OH· coordinated with the ZnPor competing with methylene blue, so the degradation rate declined sharply. We also observed a modest rebound in the degradation rate between pH 9 and 12 due to the reaction of the dye molecules with hydroxyl ions (OH-); this led to the generation of the intermediates, which easily degraded.

We also investigated the effect of the temperature on the degradation of methylene blue. The experimental results are shown in Figure 6(b). As indicated, the degradation rate of methylene blue exhibited a slight change below 25°C. However, the degradation rate clearly increased when the temperature was increased further to a peak value of 72% at 29°C, which was slightly below the LCST of ZnPor–PAM. This behavior was attributed to the alteration of the polymer chain to form a range of micellelike structures from random coils as the temperature approached the LCST.[35,36] During this transition, the concentration of the active center ZnPor was higher. On the other hand, methylene blue and H_2O_2 were encapsulated by the micellelike structure, which reduced the distance between the two species; this promoted the synergistic effect between H_2O_2 and the active center ZnPor. However, *D* gradually declined as the temperature increased further because of the precipitation of ZnPor–PAM from the aqueous solution as the temperature exceeded the LCST. The system was heterogeneous, and the active center ZnPor was embedded by PNIPAM chains, so *D* gradually declined.

Furthermore, we studied how the molecular weight affected *D* by fixing the temperature of the photocatalytic experiments at the LCST. As shown in Figure 7, the degradation rate rose sharply with increasing molecular weight, reaching approximately 91% at a molecular weight of 7800. There were two possible reasons for this phenomenon. First, the temperature (LCST) of the photocatalytic system rose as the molecular weight increased, so the molecular movement was intensified, and this facilitated the oxidative degradation of methylene blue. Second, the molecular weight was much larger, and methylene

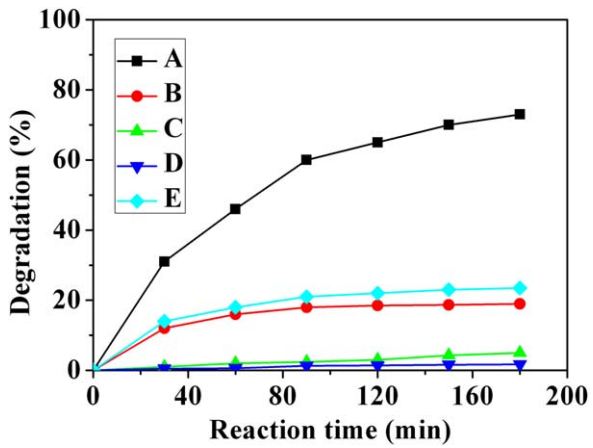

Figure 5. Kinetic curves of the photocatalytic degradation of methylene blue under various conditions at 29°C: (A) ZnPor–PAM, H_2O_2, and visible light; (B) H_2O_2 and visible light; (C) ZnPor–PAM and H_2O_2; (D) ZnPor–PAM and visible light; and (E) ZnPor–OH, H_2O_2, and visible light. The experimental conditions were as follows: methylene blue concentration = 4×10^{-5} mol/L, ZnPor–PAM (M_n = 7800) concentration = 2×10^{-5} mol/L, H_2O_2 concentration = 40 mL/L, pH = 2, and $\lambda > 450$ nm. [Color figure can be viewed in the online issue, which is available at wileyonlinelibrary.com.]

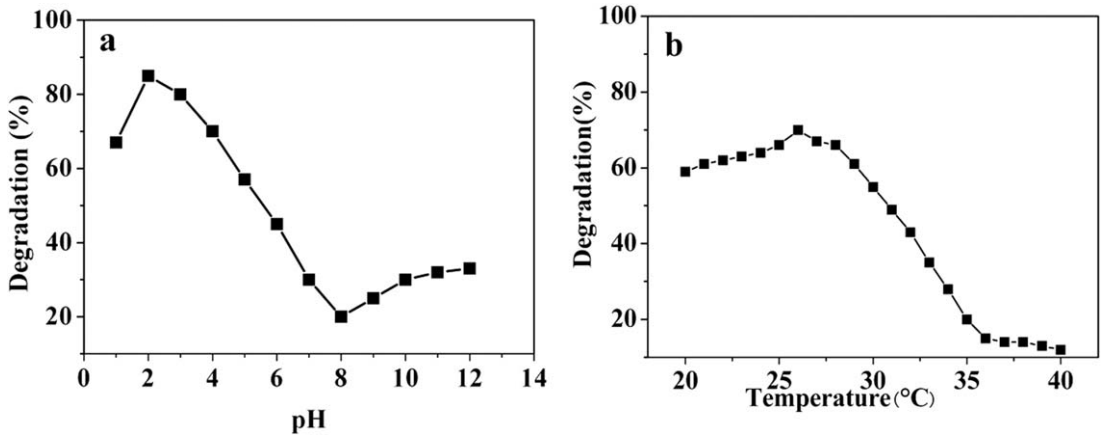

Figure 6. (a) Degradation of methylene blue at different pH values after 190 min at 29°C. The other experimental conditions were as follows: methylene blue concentration = 4×10^{-5} mol/L, ZnPor–PAM ($M_n = 7800$) concentration = 2×10^{-5} mol/L, H_2O_2 concentration = 40 mL/L, and $\lambda > 450$ nm. (b) Effect of the temperature on the degradation of methylene blue after 120 min under visible light ($\lambda > 450$ nm). The other experimental conditions were as follows: methylene blue concentration = 4×10^{-5} mol/L, ZnPor–PAM ($M_n = 7800$) concentration = 2×10^{-5} mol/L, H_2O_2 concentration = 40 mL/L, and pH = 2.

blue and H_2O_2 were better encapsulated by the micellelike structures, which improved the efficiency of degradation. However, when the molecular weights reached 10,300 and 13,100, the degradation rate decreased from its original value because the polymer chains were much too long. The active center ZnPor was embedded or methylene blue and H_2O_2 were encapsulated by the PNIPAM chains, which hindered the synergistic effect between H_2O_2 and the active center ZnPor; thus, the degradation rate decreased correspondingly.

We summarized the best experimental conditions through previous experiments. Figure 8 illustrates the changes in the UV–vis spectrum of methylene blue with irradiation time. The figure shows that the concentration of methylene blue gradually decreased with increasing reaction time. The characteristic peak of methylene blue decreased rapidly and nearly disappeared after 190 min. Concomitantly, the color of the reaction solution changed from an initial blue color to a light, transparent color, as shown in Figure 8. However, the characteristic absorption peaks of ZnPor–PAM at 430 nm remained unchanged with increasing reaction time; this suggested that the polymeric catalyst was relatively stable throughout the degradation process.

At last, the reusability and stability of ZnPor–PAM was evaluated. After the degradation of methylene blue was finished with the use of fresh catalyst (ZnPor–PAM), the used catalyst could be isolated by simple filtration because ZnPor–PAM was thermoresponsive and could agglomerate in water when the temperature was increased over its LCST. Then, the sample was washed with water several times until the filter liquor was neutral, and then, it was dried at 60°C *in vacuo* overnight. The recovered catalyst was added to a fresh solution of methylene blue, and the second cycle was carried out under the same

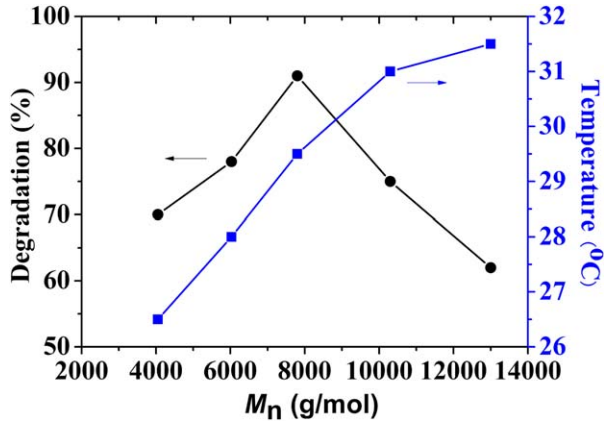

Figure 7. Degradation of methylene blue with different molecular weights after 190 min at the LCST of the polymers. The other experimental conditions were as follows: methylene blue concentration = 4×10^{-5} mol/L, ZnPor–PAM concentration = 2×10^{-5} mol/L, H_2O_2 concentration = 40 mL/L, and $\lambda > 450$ nm. [Color figure can be viewed in the online issue, which is available at wileyonlinelibrary.com.]

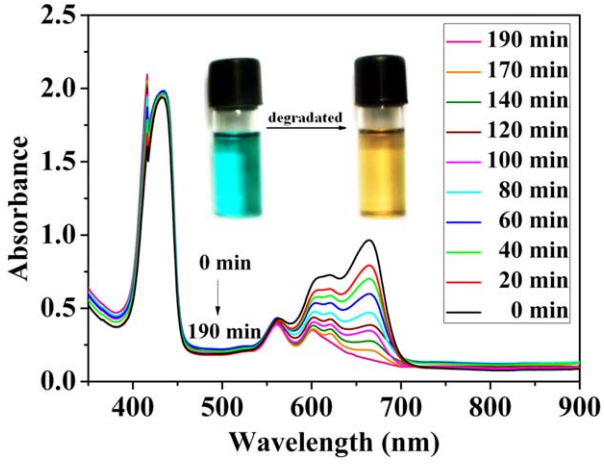

Figure 8. UV–vis spectral changes for methylene blue (initial concentration = 4×10^{-5} mol/L) as a function of the irradiation time at 29°C [ZnPor–PAM ($M_n = 7800$) concentration = 2×10^{-5} mol/L, H_2O_2 concentration = 40 mL/L, pH = 2, and $\lambda > 450$ nm]. [Color figure can be viewed in the online issue, which is available at wileyonlinelibrary.com.]

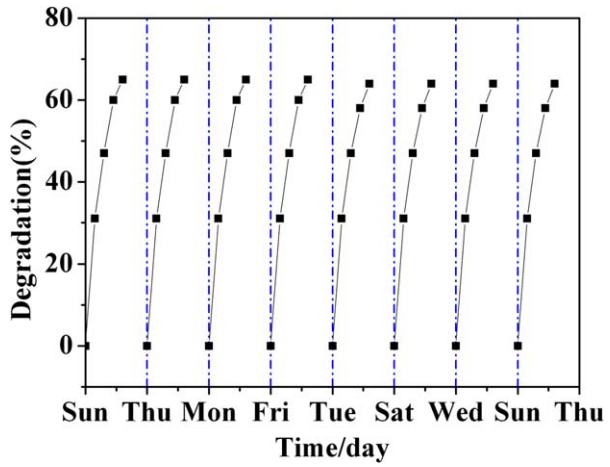

Figure 9. Recycling experiments with the catalyst ZnPor–PAM for the photocatalytic degradation of methylene blue aqueous solutions under visible light ($\lambda > 450$ nm). The experimental conditions were as follows: methylene blue concentration = 4×10^{-5} mol/L, ZnPor–PAM ($M_n = 7800$) concentration = 2×10^{-5} mol/L, H_2O_2 concentration = 40 mL/L, and pH = 2. [Color figure can be viewed in the online issue, which is available at wileyonlinelibrary.com.]

conditions. These steps were repeated seven times, and the results are shown in Figure 9. We found that the degradation rates of methylene blue were almost kept stable around 70%. So from the previous experimental results, we inferred that the ZnPor–PAM had excited photocatalytic degradation and was a convenient recycling process without secondary pollution.

Compared with some typical technologies of AOPs, such as UV/H_2O_2 and UV/TiO_2, the ZnPor–PAM/H_2O_2 could have had photocatalytic processes under visible-light irradiation, and we knew that UV light only has an average of about 5% part of the solar spectrum, whereas visible has an average of 45% abundance.[37–40] Furthermore, the ZnPor–PAM catalyst could be reused several times by simple heating and filtration without losing its catalytic activity. Therefore, this novel photocatalyst ZnPor–PAM could be favorable for potential applications in practical wastewater treatment.

CONCLUSIONS

In this study, a novel linear ZnPor–PAMs was successfully synthesized via ATRP. The PDI of the polymers indicated that the molecular weight distribution was narrow and that the polymerization was well controlled. The catalytic efficiency of ZnPor–PAM for the oxidative degradation of methylene blue in aqueous media was investigated, and the results show that the polymeric catalyst was highly effective in the oxidative degradation of methylene blue around its LCST. In addition, the catalyst could be reused several times without losing its catalytic activity.

ACKNOWLEDGMENTS

The authors are grateful to the Jilin Science and Technology Department (contract grant numbers 20070556 and 20140204017GX), the Science and Technology Bureau of Changchun City Project (contract grant numbers 2008280 and 2013060), and the Foundation for Strategic Research for their financial support.

REFERENCES

1. Panniello, A.; Curri, M. L.; Diso, D.; Licciulli, A.; Locaputo, V.; Agostiano, A.; Comparelli, A.; Mascolo, G. *Appl. Catal. B* **2012**, *121*, 190.
2. Vandevivere, P. C.; Bianchi, R.; Verstraete, W. *J. Chem. Technol. Biotechnol.* **1998**, *72*, 289.
3. Bhatnagar, A.; Vilar, V. J.; Botelho, C. M.; Boaventura, R. A. *Environ. Technol.* **2011**, *32*, 231.
4. Chen, C.; Ma, W.; Zhao, J. *Chem. Soc. Rev.* **2010**, *39*, 4206.
5. Marin, M. L.; Santos-Juanes, L.; Arques, A.; Amat, A. M.; Miranda, M. A. *Chem. Rev.* **2011**, *112*, 1710.
6. Silva, N. U.; Nunes, T. G.; Saraiva, M. S.; Shalamzari, M. S.; Vaz, P. D.; Monteiro, O. C.; Nunes, C. D. *Appl. Catal. B* **2012**, *113*, 180.
7. Mohamed, M. M.; Al-Esaimi, M. M. *J. Mol. Catal. A* **2006**, *255*, 53.
8. Cho, K. Y.; Choi, J. W.; Lee, S. H.; Hwang, S. S.; Baek, K.-Y. *Polym. Chem.* **2013**, *4*, 2400.
9. Zhang, F.; Zhao, J.; Shen, T.; Hidaka, H.; Pelizzetti, E.; Serpone, N. *Appl. Catal. B* **1998**, *15*, 147.
10. Páez, C. A.; Lambert, S. D.; Poelman, D.; Pirard, J. P.; Heinrichs, B. *Appl. Catal. B* **2011**, *106*, 220.
11. Houas, A.; Lachheb, H.; Ksibi, M.; Elaloui, E.; Guillard, C.; Herrmann, J. M. *Appl. Catal. B* **2001**, *31*, 145.
12. Shen, X.; Lu, W.; Feng, G.; Yao, Y.; Chen, W. *J. Mol. Catal. A* **2009**, *298*, 17.
13. Zhao, P.; Woo, J. W.; Park, Y. S.; Song, Y.; Zhang, F. *Macromol. Res.* **2010**, *18*, 496.
14. Yamazaki, A.; Song, J. M.; Winnik, F. M.; Brash, J. L. *Macromolecules* **1998**, *31*, 109.
15. Ankareddi, I.; Brazel, C. S. *Int. J. Pharm.* **2007**, *336*, 241.
16. Fujimoto, K.; Iwasaki, C.; Arai, C.; Kuwako, M.; Yasugi, E. *Biomacromolecules* **2000**, *1*, 515.
17. Zhang, X. Z.; Zhuo, R. X.; Cui, J. Z.; Zhang, J. T. *Int. J. Pharm.* **2002**, *235*, 43.
18. Matsuda, T.; Saito, Y.; Shoda, K. *Biomacromolecules* **2007**, *8*, 2345.
19. Pennadam, S. S.; Lavigne, M. D.; Dutta, C. F.; Firman, K. D.; Mernagh, D. C.; Alexander, C. *J. Am. Chem. Soc.* **2004**, *126*, 13208.
20. Lu, X. J.; Zhang, L. F.; Meng, L. Z.; Liu, Y. H. *Polym. Bull.* **2007**, *59*, 195.
21. Schulte, T.; Siegenthaler, K. O.; Luftmann, H.; Letzel, M.; Studer, A. *Macromolecules* **2005**, *38*, 6833.
22. Masci, G.; Giacomelli, L.; Crescenzi, V. *Macromol. Rapid Commun.* **2004**, *25*, 559.
23. Wang, J. S.; Matyjaszewski, K. *J. Am. Chem. Soc.* **1995**, *117*, 5614.
24. Kato, M.; Kamigaito, M.; Sawamoto, M.; Higashimura, T. *Macromolecules* **1995**, *28*, 1721.
25. Duan, Q.; Narumi, A.; Miura, Y.; Shen, X. D.; Sato, S. I.; Satoh, T.; Kakuchi, T. *Polym. J.* **2006**, *38*, 306.
26. Duan, Q.; Miura, Y.; Narumi, A.; Shen, X. D.; Sato, I. S.; Satoh, T.; Kakuchi, T. *J. Polym. Sci. Part A: Polym. Chem.* **2006**, *4*, 1117.

27. Tao, X. D.; Gao, Z. G.; Satoh, T.; Cui, Y.; Kakuchi, T.; Duan, Q. *Polym. Chem.* **2011**, *2*, 2068.

28. Gao, Z. G.; Tao, X. D.; Cui, Y.; Satoh, T.; Kakuchi, T.; Duan, Q. *Polym. Chem.* **2011**, *2*, 2590.

29. Ciampolini, M.; Nardi, N. *Inorg. Chem.* **1966**, *5*, 41.

30. Barkigia, K. M.; Berber, M. D.; Fajer, J.; Medforth, C. J.; Renner, M. W.; Smith, K. M. *J. Am. Chem. Soc.* **1990**, *112*, 8851.

31. Xia, Y.; Yin, X. C.; Burke, N. A. D.; Stvover, H. D. H. *Macromolecules* **2005**, *38*, 5937.

32. Bonnett, R. *Chem. Soc. Rev.* **1995**, *24*, 19.

33. Yao, G. P.; Li, J.; Luo, Y.; Sun, W. J. *J. Mol. Catal. A* **2012**, *361*, 29.

34. Zhang, Z. H.; Zhang, M. J.; Deng, J.; Deng, K. J.; Zhang, B. G.; Lv, K.; Sun, J.; Chen, L. Q. *Appl. Catal. B* **2013**, *132*, 90.

35. Chen, W.; Zhao, B.; Pan, Y.; Yao, Y.; Lu, S.; Chen, S.; Du, L. *J. Colloid Interface Sci.* **2006**, *300*, 626.

36. Chen, W. X.; Lv, W. Y.; Shen, X. Y.; Yao, Y. Y. *Sci. China Chem.* **2010**, *53*, 638.

37. Rahimi, R.; Moghaddas, M. M.; Zargari, S. *J. Sol-Gel Sci. Technol.* **2013**, *65*, 420.

38. Park, D. J.; Sekino, T. S.; Tanaka, T. S. I. *Res. Chem. Intermed.* **2013**, *39*, 1581.

39. Barnes, R. J.; Molina, R.; Xu, J. B.; Dobson, P. J.; Thompson, I. P. *J. Nanopart. Res.* **2013**, *15*, 1432.

40. Dai, K.; Lu, L. H.; Dawson, G. *J. Mater. Eng. Perform.* **2013**, *22*, 1035.